

Frequency and temperature dependent transport properties of NiCuZn ceramic oxide

M. BELAL HOSSEN^{1*}, A.K.M. AKTHER HOSSAIN²

¹Department of Physics, Chittagong University of Engineering and Technology, Bangladesh

²Department of Physics, Bangladesh University of Engineering and Technology, Bangladesh

A polycrystalline sample of ceramic oxide $\text{Ni}_{0.27}\text{Cu}_{0.10}\text{Zn}_{0.63}\text{Fe}_2\text{O}_4$ was prepared by the solid state reaction method. The sintered sample was well polished to remove any oxide layer formed during sintering and the two surfaces of the pellet were coated with a silver paste as a contact material. Among dielectric properties, complex dielectric constant ($\epsilon^* = \epsilon' - j\epsilon''$), loss tangent ($\tan\delta$) and ac conductivity (σ_{ac}) in the frequency range of 20 Hz to 2 MHz were analyzed in the temperature range of 303 to 498 K using a Wayne Kerr impedance analyzer (model No. 6500B). The experimental results indicate that ϵ' , ϵ'' , $\tan\delta$ and σ_{ac} decrease with an increase in frequency and increase with increasing temperature. The transition temperature, as obtained from dispersion curve of ϵ' , shifts towards higher temperature with an increase in frequency. The variation of dielectric properties with frequency and temperature shows the dispersion behavior which is explained in the light of Maxwell-Wagner type of interfacial polarization in accordance with the Koop's phenomenological theory. The frequency dependent conductivity results satisfy the Jonscher's power law, $\sigma_T(\omega) = \sigma(\infty) + A\omega^n$, and the results show the occurrence of two types of conduction process at elevated temperature: (i) low frequency conductivity, due to long-range ordering (frequency independent, region I), (ii) mid frequency conductivity at the grain boundaries (region II, dispersion) and (iii) high frequency conductivity at the grain interior due to the short-range hopping mechanism (frequency independent plateau, region III).

Keywords: NiCuZn ferrite; dielectric properties; ac conductivity; frequency and temperature dependence

© Wrocław University of Technology.

1. Introduction

The current decade has witnessed vast research interest in ferrites, which achieved a prime position of economic and technological importance within the family of magnetic ceramic oxides because of their excellent physical properties [1–5]. The physical properties of ferrites are controlled by the preparation conditions, chemical composition, sintering temperature and time, type and amount of substitutions [6]. Various physical properties of polycrystalline ferrites are highly influenced by distribution of cations among the sub lattices, nature of grain (shape, size, and orientation), grain boundaries, voids, inhomogeneities, surface layers, contacts etc. [7–9]. The information about the associated physical parameters of the microstructural components is important since the overall

properties of the materials are determined by these components. An important characteristics of ferrites is their high value of resistivity and low eddy current losses [10–12], which make them ideal for high frequency applications.

For microwave applications, the dielectric properties, such as dielectric constant and dielectric loss, are very important as the dielectric constant affects the thickness of microwave absorbing layer and the dielectric loss factor ($\tan\delta$) of a material determines dissipation of the electrical energy. This dissipation may be due to electrical conduction, dielectric relaxation, dielectric resonance and loss from non-linear processes. Due to the combined effect of electrical and magnetic properties of ferrites, they are good candidates as multiferroic materials. Recently, Kumar et al. have reported that ferrites also behave like multiferroics [13].

Dispersion in dielectric constant and loss tangent with frequency in polycrystalline ferrites

*E-mail: belalcuet@gmail.com

is strongly dependent on the polarization process [14], and is also related to the conduction mechanism [15]. The aim of the present work is to study the mechanism of dielectric polarization and conduction as a function of frequency and temperature.

2. Experimental

NiCuZn ferrite of $\text{Ni}_{0.27}\text{Cu}_{0.10}\text{Zn}_{0.63}\text{Fe}_2\text{O}_4$ system was prepared by a standard solid state reaction technique at Solid State Physics Laboratory, Department of Physics, Bangladesh University of Engineering and Technology (BUET), Dhaka, Bangladesh. The starting materials were in the form of AR grade oxides (Fe_2O_3 , NiO, CuO and ZnO) from E. Merck, Germany. The reagent powders were weighed precisely according to their molecular weight. Homogeneous mixing of the materials was carried out using an agate mortar in acetone media for 4 h. These powders were calcined at 1173 K for 5 h at a heating rate of $10 \text{ K}\cdot\text{min}^{-1}$ in air to form ferrite through chemical reaction, and then cooled down to room temperature at a cooling rate of $5 \text{ K}\cdot\text{min}^{-1}$. The calcined materials were crushed for another 1 h in acetone to reduce it to small crystallites of uniform size. The mixture was dried and a small amount of saturated solution of polyvinyl alcohol was added as a binder. The resulting powders were pressed uniaxially under a pressure of 55.18 MPa in a stainless steel die to make pellets.

The pressed pellet was then finally sintered at 1573 K for 5 h in air. The surfaces of the sample were well polished in order to remove any oxide layer formed during the process of sintering and the two surfaces of the pellet were coated with a silver paste as a contact material for electrical and dielectric measurements. Dielectric measurement as a function of frequency in the range of 20 Hz to 2 MHz at room temperature and also as a function of temperature in the range of 303 to 498 K at different frequencies were carried out using Waynekerr impedance analyzer (model No. 6500B) in conjunction with a computer controlled furnace, which maintained the desired temperature with the help of a programmable temperature controller. The real

part of dielectric constant was calculated using the formula:

$$\epsilon' = (C_p d) / (\epsilon_0 A) \quad (1)$$

where C_p is the capacitance of the pellet in F, d the thickness of the pellet in m, A is the cross sectional area of the flat surface of the pellet in m^2 and ϵ_0 – the constant of permittivity for free space which is equal to $8.85 \times 10^{-12} \text{ F/m}$.

The imaginary part of dielectric constant (ϵ'') of the sample was calculated using relation:

$$\epsilon'' = \epsilon' \times \tan \delta \quad (2)$$

where $\tan \delta$ is the dielectric loss tangent.

The frequency dependence of conductivity is expressed as: $\sigma_{AC} = d / (A \times R_{AC})$; where R_{AC} is the AC resistance.

3. Results and discussion

The X-ray diffraction (XRD) pattern for a $\text{Ni}_{0.27}\text{Cu}_{0.10}\text{Zn}_{0.63}\text{Fe}_2\text{O}_4$ sample is shown in Fig. 1a. The XRD pattern, without any extra lines that would not belong to the spinel structure, provides a clear evidence of single phase spinel structure formation. It is obvious that the peaks characteristic of spinel NiCuZn ferrite appear in the diffractogram as the main crystalline phase in the sample. The peaks (1 1 1), (2 2 0), (3 1 1), (2 2 2), (4 0 0), (4 2 2), (5 1 1) and (4 4 0) correspond to spinel phase.

The lattice parameter was determined by the Nelson-Riley extrapolation method. The values of the lattice parameter obtained from each reflected plane have been plotted against Nelson-Riley function [13]:

$$F(\theta) = 1/2[\cos^2 \theta / \sin \theta + \cos^2 \theta / \theta] \quad (3)$$

where θ is the Bragg's angle at which the straight line is obtained. The good matching of the lattice parameter vs. $F(\theta)$ with a straight line also confirms the single phase character of the material (Fig. 1b). The accurate value of the lattice constant was estimated from the extrapolation of the line to $F(\theta) = 0$ or $\theta = 90^\circ$.

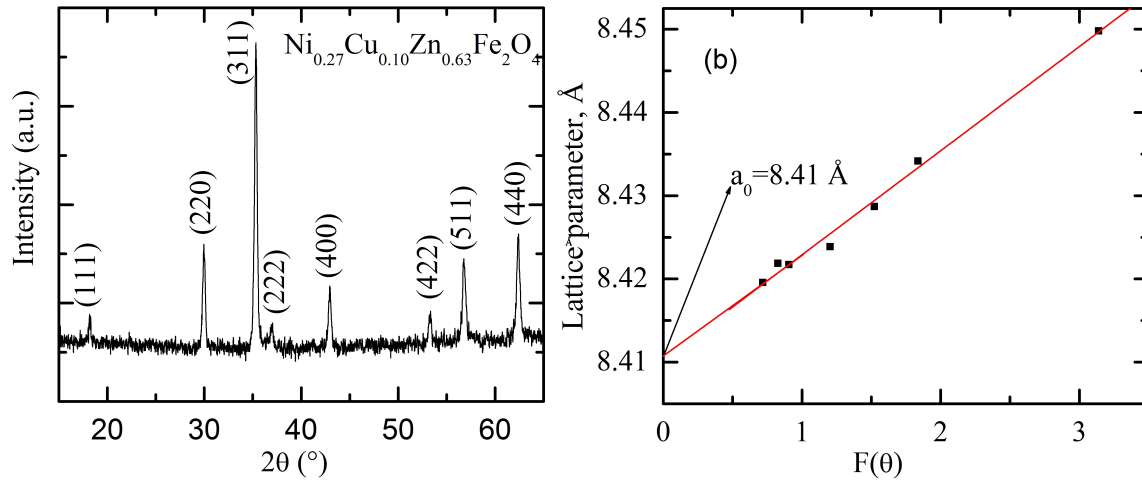


Fig. 1. XRD pattern of $\text{Ni}_{0.27}\text{Cu}_{0.10}\text{Zn}_{0.63}\text{Fe}_2\text{O}_4$ (a) and N-R function of ceramics at room temperature (b).

Fig. 2 shows the variation of ϵ' and ϵ'' with frequency from 20 Hz to 2 MHz at different measuring temperatures (T_{SM}), selected from the range of 303 to 498 K. It can be seen that at all temperatures the sample shows the frequency-dependent phenomena, i.e. the dielectric constant decreases with increasing frequency exhibiting a normal ferromagnetic behavior. The value of dielectric constant rapidly decreases at the region of low frequency, further at the region of middle frequency, but the rate of decreasing is significantly smaller, and at the high frequency range the dependency becomes almost constant. The value of ϵ'' decreases faster (Fig. 2b) than ϵ' (Fig. 2a) and tends to the same value in the high frequency range. The dielectric behavior of ferrites may be explained on the basis of dielectric polarization process, which is similar to that of the conduction mechanism and is caused mainly by the hopping conduction mechanism. Electrical conduction in ferrites can be explained by Verwey-de-Boer hopping mechanism [16]. Verwey explained that the electrical conduction in ferrites is mainly due to hopping of electrons between ions of the same element existing in more than one valence state and distributed randomly over crystallographically equivalent lattice (octahedral sites, due to smaller distances between the cations) sites. In the present case it has been found that the dielectric constant decreases gradually at lower frequencies and remains almost

constant at higher frequencies, indicating dielectric dispersion. The dielectric constant decreases with increasing frequency and then reaches a constant value due to the fact that beyond a certain frequency of an external ac field, the electron exchange between Fe^{2+} and Fe^{3+} is not able to follow the alternating field. The dispersion of ϵ' can also be explained based on the contributions from various sources of polarizations [17, 18]. The larger value of ϵ' at lower frequencies is attributed to four types of polarization: space charge/interface (grain-boundaries), dipolar, atomic and electronic, however, dipolar and interfacial polarizations are known to play the dominant role. Space charge polarization is due to the accumulation of charges at the grain boundaries; an increase in polarization occurs as more and more charges reach the grain boundary with an increase in temperature. The decrease (and finally disappearance) in ionic and orientation polarizability as well as release of space charge polarization with increasing frequency may be responsible for the decrease in ϵ' at higher frequencies [19]. Fig. 2a correlates the ϵ' and frequency of the sample at T_{SM} . The value of ϵ' is increasing with T_{sm} . It is also observed that the value of ϵ' is shifting to higher frequency side with T_{sm} which might be due to the contribution of space charges increased with T_{sm} . The contribution of ϵ' at high frequency side also increases proportionally with T_{SM} (inset of Fig. 2a). The rates of

increasing dissipation energy (ϵ'') in the measured frequency range are similar for all the T_{SM} (inset of Fig. 2b). With increasing temperature the number of charge carriers increases, resulting in enhanced buildup of space charge polarization governed by space charge carriers. Hence, the values of dielectric parameters increase. The high value at lower frequency region is due to Maxwell-Wagner interfacial type of polarization [20, 21] for the inhomogeneous double layer dielectric structure, which is in agreement with Koop's phenomenological theory [22]. The inhomogeneous dielectric structure was supposed to be consisted of two layers. The first one contains the fairly well conducting large ferrite grains which are separated by the second thin layer of the poorly conducting grain boundaries. The grain boundaries of low conductivity and high dielectric constant are found to be more effective at lower frequencies, while the ferrite grains of higher conductivity and lower dielectric constant are more effective at high frequencies [23]. The presence of Fe^{2+} ions in excess amount favors the polarization effects. Thus, the higher dispersion observed in the samples can be attributed to the presence of Fe^{2+} ions in excess amount which could be formed at elevated measuring temperature. Since in ceramic oxide the rotational displacement of $Fe^{3+} \leftrightarrow Fe^{2+}$ dipoles results in orientational polarization that may be visualized as exchange of electrons between the ions, the dipoles align themselves along the alternating field. In the studied material the presence of Ni^{2+}/Ni^{3+} and Cu^{2+}/Cu^{+} ions gives rise to p-type carriers, and their displacement in the direction of external electric field also contributes to the net polarization, in addition to that of n-type carriers. However, the contribution due to p-type carriers is smaller than the electronic exchange between Fe^{3+} and Fe^{2+} ions and has an opposite sign since the mobility of p-type carriers is smaller than that of n-type carriers. As a result, net polarization increases initially and then decreases with increasing frequency. This may be attributed to polarization due to changes in valence states of cations and space charge polarization. At higher frequencies the dielectric constant does not change; it may be due to the inability of electric dipoles to follow up the fast variation of the applied

alternating electric field. Consequently, the occurrences of friction between dipoles dissipate energy in the form of heat. In turn, this affects the internal viscosity of the system and decreases the dielectric constant. These frequency independent values are known as static values of the dielectric constant. Similar results were reported earlier by Popandian et al. [24].

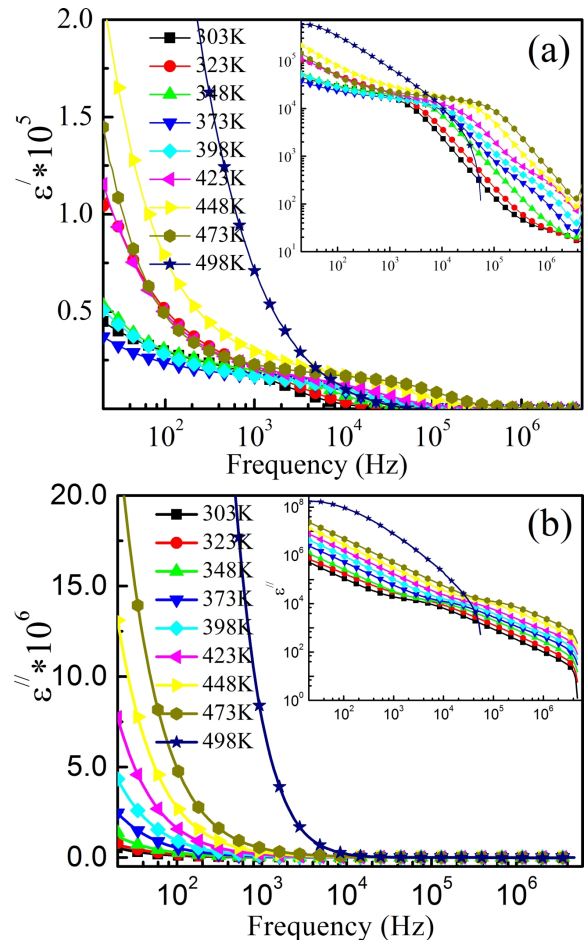


Fig. 2. Variation of (a) ϵ' and (b) ϵ'' with frequency at T_{SM} for $Ni_{0.27}Cu_{0.10}Zn_{0.63}Fe_2O_4$.

Fig. 3 shows the temperature dependence of dielectric constant at selected frequencies, which is the essential part of our study. In general, ϵ' and ϵ'' increase as the temperature increases, indicating the semiconducting nature of the ceramic oxide. The dielectric dispersion of ϵ' and ϵ'' is weak in low-temperature region. It can be explained on the basis that at relatively low temperature, the

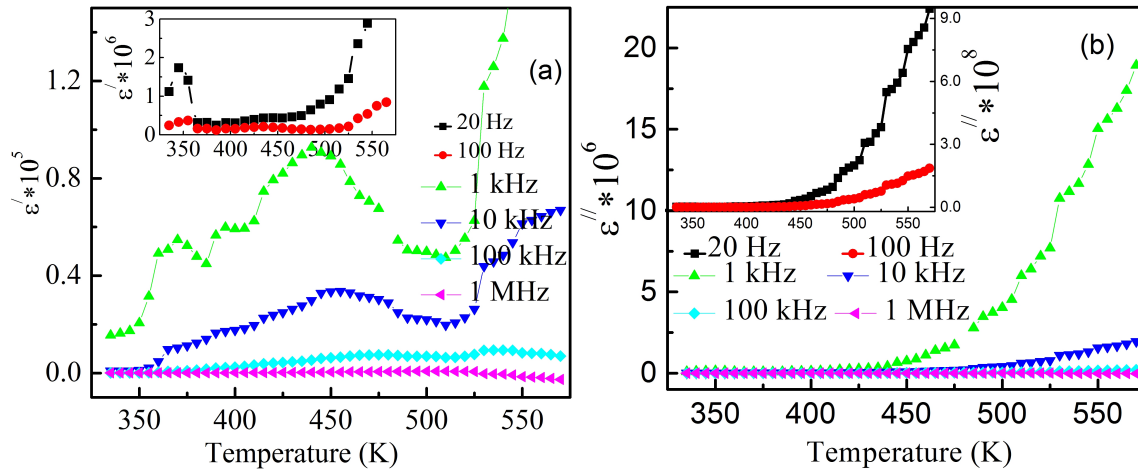


Fig. 3. Variation of (a) ϵ' and (b) ϵ'' with temperature at different frequencies for $\text{Ni}_{0.27}\text{Cu}_{0.10}\text{Zn}_{0.63}\text{Fe}_2\text{O}_4$.

charge carriers in most cases are not able to orient themselves with respect to the direction of applied field; therefore, they have a weak contribution to the polarization and the dielectric behavior. As the temperature increases, the bond charge carriers get enough thermal excitation energy to be able to obey the change in the external field more easily. These thermal excitations of atoms about their lattice points may be due to disorder at the lattice. Space charge contribution to the polarization may be attributed to the thermally activated charge carriers. This, in turn, enhances their contribution to the polarization, leading to an increase of dielectric constant.

Further, it is clear that the ϵ' for all measured temperatures shows a peak at a characteristic temperature (relaxation processes) depending on the selected frequencies. This phenomenon, i.e. dielectric anomaly, is referred as the ferroelectric-paraelectric transition. The peaks are found to be shifted to higher temperature as the frequency increases. These peaks appear when the jumping frequency of localized electron approximately becomes equal to that of the externally applied ac electric field frequency. It can be seen that in all the systems the transition is of diffuse type. It is well known that the process in the oxygen-rich ambient decreases the density of oxygen vacancies and reversely, the process in the oxygen-deficient ambient increases the density of oxygen vacancies in the samples. So, the relaxation peak is considered to

be associated with the oxygen vacancies. Another interesting phenomenon is that the peak tends to be broadened and unanimously shifted towards the high temperature. It indicates that the peak belongs to relaxation type peaks. There is a wide consensus that the anomaly appearing in the high temperature range in oxide materials is related to oxygen vacancies [25]. This suggests that the high-temperature anomaly in our sample may be related to oxygen vacancies. The increase in ϵ' with temperature has earlier been observed for the Mg-Ti [26], Ni-Zn [27], Mg-Zn [28] ferrites. The hopping of electrons between Fe^{2+} and Fe^{3+} ions at adjacent B-sites is thermally activated on increasing the temperature. The hopping of these strongly localized electrons in the d-shell causes local displacements in the direction of applied ac field. The local displacements of electronic charge carriers cause the dielectric polarization in ferrites. In the first region ϵ' is increasing slowly with temperature. This may be due to the fact that the thermal energy supplied to the system is not sufficient to free the localized dipoles and to orient them in the field direction. In most cases, the atoms or molecules in the samples cannot orient themselves at a low temperature region. When the temperature rises, the orientation of these dipoles is facilitated and this increases the dielectric polarization. At very high temperatures the chaotic thermal oscillations of molecules are intensified and the dielectric constant passes through a maximum value. It is

observed that the variation of dielectric constant with temperature at lower frequencies is much more pronounced than at higher frequencies.

Fig. 4 shows variation of loss tangent ($\tan\delta$) with temperature. The values of $\tan\delta$ increase with increasing frequency and temperature. Loss tangent or $\tan\delta$ represents the energy dissipation in the dielectric system. In general, $\tan\delta$ in polycrystalline ferrites is a result of the lag in polarization with respect to the applied alternating electric field. Moreover, the loss factor is considered to be caused by domain wall resonance. At higher frequencies, losses are found to be low since the domain wall motion is inhibited and magnetization is forced to change by rotation [29]. In the low frequency region, it is considered to be caused by phase lagging of space charge polarization with applied field frequency.

Fig. 4a shows the variation in $\tan\delta$ with frequency at T_{SM} . With increasing T_{SM} , $\tan\delta$ also increases and the range of frequency up to which $\tan\delta$ becomes minimum also increases. As $\tan\delta$ is proportional to the ϵ'' , so it exhibits similar dispersion behavior. It is also observed from the plots that the higher dielectric loss occurs at higher temperature and lower frequencies. This is understandable from the fact that at lower frequencies the trend is due to space charge polarization and at higher temperatures the trend may be due to macroscopic distortion of charges [30].

The variation of dielectric loss at low frequencies with respect to temperature and frequency may be due to space charge polarization [31]. Further, the space charge polarization can be explained through Shockley-Read mechanism. This mechanism assumes that at low and middle order frequencies and at higher temperatures the impurity ions in the bulk crystal matrices capture the surface electrons, causing the space charge polarization at the surfaces. The electron capture process increases with an increase in temperature. By this mechanism, one can consider that the loss tangent increases with increasing temperature and at low frequencies [32].

Fig. 5 illustrates the curves correlating the temperature dependence of the ac-conductivity

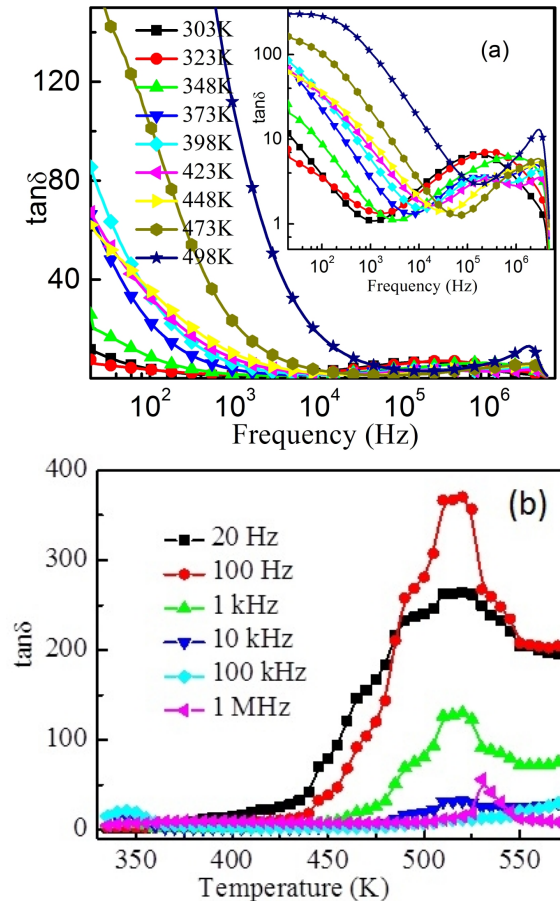


Fig. 4. Variation of $\tan\delta$ with (a) frequency and (b) temperature at different selected temperatures and frequencies, respectively, for $\text{Ni}_{0.27}\text{Cu}_{0.10}\text{Zn}_{0.63}\text{Fe}_2\text{O}_4$.

(σ_{AC}) for the investigated ferrite. From the figure it is clear that as the frequency increases σ_{AC} exhibits a step-like increment which is characteristic of a potential profile with multiple activation energies. The increase in σ_{AC} with the applied frequency can be explained on the basis of barrier hopping conduction mechanism due to bound charge carriers. The crossover frequency from region I to II was found to increase with temperature, and at $T_{SM} = 498$ K region II disappears. The frequency independent plateau at lower frequencies and high temperatures may be associated to the activated hopping of charge carriers to the adjacent vacant lattice sites, resulting in long range translational motion of charge carriers, giving rise to dc conductivity. At the high frequency, short range translational

motion of charge carriers takes place. Above these frequencies there is a third region formed, where reorientational hopping motion takes place. In order to investigate the σ_{AC} at a constant temperature we can use the universal power relation – an elegant tool proposed by Jonscher [33] as:

$$\sigma_T(\omega) = \sigma(o) + A\omega^n \quad (4)$$

where $\sigma(0)$ is the frequency independent conductivity, A is the temperature dependent pre-factor, and n is the frequency exponent. The variations of $\sigma_T(\omega)$ with frequency, for T_{SM} , are shown in Fig. 5a in log-log form. A frequency-independent plateau appears for the low frequency range, associated with the term $\sigma(o)$. The term $A\omega^n$ contains the ac dependence and characterizes all dispersion phenomena. To understand the conductivity of these types of oxides the second term individually accounts for different regimes. The conductivity at lower frequencies may be approximated as dc conductivity, and in region II, dispersion is observed at lower frequencies, while a plateau at higher frequencies. The dispersion region accounts for the ac conductivity of the grain boundaries and the plateau region for the dc conductivity of grains. The frequency dispersion (region II) corresponds to a short range translational hopping mechanism.

Fig. 5b shows the temperature dependence of σ_{AC} at different selected frequencies. As the temperature increases, σ_{AC} also increases, which is clear from Fig. 5a. As ferrites exhibit semiconducting behavior, the σ_{AC} of ferrites increases with increasing temperature according to the well known Arrhenius equation:

$$\sigma_{AC} = \sigma_0 \exp \left[-\frac{E_a}{k_B T} \right] \quad (5)$$

where E_a represents the activation energy, σ_{AC} is the conductivity at temperature T , σ_0 is a temperature independent constant and k_B is the Boltzmann constant. The apparent E_a at different frequencies is determined by plotting $\ln(\sigma_{AC})$ vs $1/T$ as shown in Fig. 5b (inset). The inset also shows the low and high-temperature frequency-dependent conductivity based activation energies of the sample. From Fig. 5b it is clear that the E_a

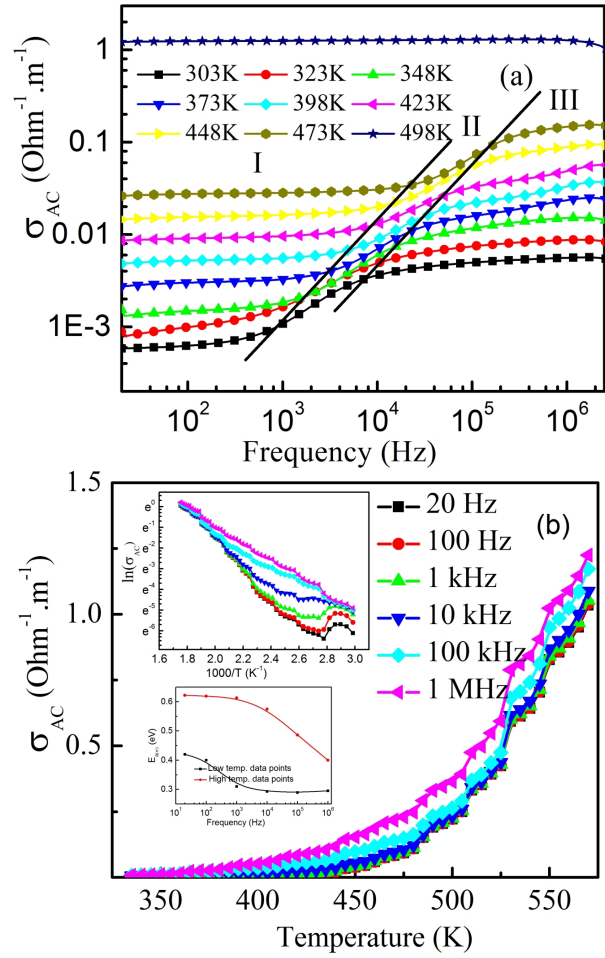


Fig. 5. Variation of σ_{AC} with (a) frequency and (b) temperature at different selected temperatures and frequencies, respectively, for $Ni_{0.27}Cu_{0.10}Zn_{0.63}Fe_2O_4$.

values at high temperature region are greater than that of low temperature one for all measured frequencies. This frequency dependent activation energy results from the multiple site hopping conduction mechanism and the trend of decreasing in activation energy with an increase in frequency is observed in the entire temperature range. This conductivity discussion is consistent with the Mott's theory [34], which states that at low temperatures, the hopping range can be much larger than the distance between the neighboring equivalent sites due to the lower activation energy involved. The larger E_a might be due to magnetic transition as explained by Goodenough [35]. According to him, the mag-

netic transition can be considered as a second order one, which is characterized by a large temperature range. This second order transition may be due to volume expansion, i.e. an increase in the jumping length between the ions, hence, an increase in E_a . The temperature dependent σ_{AC} suggests that the conduction process is thermally assisted [36].

4. Conclusions

The magnetic ceramic oxides consisting of $Ni_{0.27}Cu_{0.10}Zn_{0.63}Fe_2O_4$ have been prepared by a standard solid state reaction technique. The dielectric constant and dielectric loss decreased, while the ac conductivity increased as the frequency increased for all the measuring temperatures. The dielectric dispersion with frequency has been explained on the basis of electron-hole hopping mechanism, which is responsible for conduction and polarization. The temperature dependent dielectric constant showed peaking behavior and the peaking happened at higher temperature, depending on the increasing selected frequencies. The dielectric losses were reflected in the conductivity measurements, where the materials of high conductivity exhibited high losses and vice versa. The parameters ϵ' , ϵ'' , $\tan\delta$ and σ_{AC} increased with the rise in temperature due to increase in mobility and thermal activation of hopping frequency. The conductivity spectra obey well the modified Jonscher's power law, indicating different contributions to the conductivity; the low frequency conductivity is due to the long-range translational hopping of charge carriers at the grain boundaries and above the crossover frequency, conductivity is dominated by the short-range translational hopping motion. The ac conductivity data were used to evaluate the apparent activation energy.

Acknowledgements

The authors gratefully acknowledge CASR of Bangladesh University of Engineering and Technology (BUET) for financial support for this research.

References

- [1] KÖSEOĞLU Y., KAVAS H., *J. Nanosci. Nanotechnol.*, 8 (2008), 584.

- [2] LIPARE A.Y., VASAMBEKAR P.N., VAINGANKAR A.S., *J. Magn. Magn. Mater.*, 279 (2004), 160.
- [3] ZI Z., SUN Y., ZHU X., YANG Z., DAI J., SONG W., *J. Magn. Magn. Mater.*, 321 (2009), 1251.
- [4] PENG J., HOJAMBERDIEV M., XU Y., CAO B., WANG J., WU H., *J. Magn. Magn. Mater.*, 323 (2011) 133.
- [5] VADIVEL M., RAMESH BABU R., SETHURAMAN K., RAMAMURTHI K., ARIVANANDHAN M., *J. Magn. Magn. Mater.*, 362 (2014), 122.
- [6] VERWEY E.J., HAAIJAM P.W., ROMEYN F.C., VAN OOSTERHOUT G.W., *Philips Res. Rep.*, 5 (1950), 173.
- [7] BATOO K.M., KUMAR S., PRAKASH R., ALIMUDDIN, SONG I., CHUNG H., JEONG H., LEE C.G., *J. Cent. South Univ.*, 17 (2010), 1129.
- [8] KUMAR S., FAREA A.M.M., BATOO K.M., LEE C.G., KOO B.H., YOUSEF A., ALIMUDDIN, *Physica B*, 403 (2008), 3604.
- [9] BATOO K.M., KUMAR S., LEE C.G., ALIMUDDIN, *J. Alloy. Compd.*, 480 (2009), 596.
- [10] YAMAMOTO Y., MAKINO, *J. Magn. Magn. Mater.*, 133 (1994), 500.
- [11] FAREA A.M.M., KUMAR S., BATOO K.M., LEE C.G., KOO B.H., YOUSEF A., *J. Alloy. Compd.*, 469 (2009), 451.
- [12] BAMMANAVAR B.K., NAIK L.R., CHOUGULE B.K., *J. Appl. Phys.*, 104 (2008), 064123.
- [13] KUMAR S., ALIMUDDIN, KUMAR R., DOGRA A., REDDY V.R., BANERJEE A., *J. Appl. Phys.*, 99 (2006), 08M910.
- [14] PATIL R.S., KAKATKAR S.V., PATIL S.A., MASKAR P.K., SAWANT S.R., *Phys. Status Solidi A*, 126 (1991), K185.
- [15] IWAUCHI K., *Jpn. J. Appl. Phys.*, 10 (1971), 1520.
- [16] VERWEY E.J.W., HAAYMAN W., *Physica*, 8 (1941), 979.
- [17] COLE K.S., COLE R.H., *J. Chem. Phys.*, 9 (1941), 341.
- [18] ANDERSON J.C., *Dielectrics*, Spottiswoode, Ballantyne & Co Ltd., London and Colchester, 1964.
- [19] SMITH J., WIJN H.P.J., *Ferrites*, Philips Technical Library, Eindhoven, The Netherlands, 1965.
- [20] MAXWELL J., *A Treatise on Electricity and Magnetism*, Clarendon Press, Oxford, London, 1982.
- [21] WANGNER K., *Ann. Phys.-Berlin*, 40 (1913), 817.
- [22] KOOPS C.G., *Phys. Rev.*, 83 (1951), 121.
- [23] KUMAR B., SRIVASTAVA G., *J. Appl. Phys.*, 75 (1994), 6115.
- [24] POPANDIAN N., BALAYA P., NARAYANASAMY A., *J. Phys.-Condens. Mat.*, 14 (2002), 3221.
- [25] ANG C., YU Z., CROSS L.E., *Phys. Rev. B*, 62 (2000), 228.
- [26] AHMED M.A., ATEIA E., SALEM F.M., *Physica B*, 381 (2006), 144.
- [27] VERMA A., KHAKUR O.P., PRAKASH C., GOEL T.C., MENDIRATTA R.G., *Mater. Sci. Eng. B-Adv.*, 116 (2005), 1.
- [28] EL HITI M.A., *J. Magn. Magn. Mater.*, 192 (1999), 305.
- [29] DEVAN R.S., KOLEKAR Y.D., CHOUGULE B.K., *J. Phys.-Condens. Mat.*, 18 (2006), 9809.

- [30] KAMBA S., BOVTUN V., PETZELT J., RYCHETSKY I., MIZARAS R., BRILINGAS A., BANYS J., GRIGAS J., KOSEC M., *J. Phys.-Condens. Mat.*, 12 (2000), 497.
- [31] DAS B.P., MAHAPATRA P.K., CHOUDHARY R.N.P., *J. Mater. Sci.-Mater. El.*, 15 (2004), 107.
- [32] KANAGATHARA N., ANBALAGAN G., REN-GANATHAN N.G., *Int. J. Sci. Tech.*, 1 (2011), 33.
- [33] JONSCHER A.K., *Nature*, 264 (1977), 673.
- [34] MOTT N.F., DAVIS E.A., *Electronic Processes in Non-crystalline Materials*, Clarendon Press, Oxford, 1979.
- [35] GOODENOUGH J.B., *Mater. Res. Bull.*, 8 (1973), 423.
- [36] PRADHAN D.K., MISRA P., PULI V.S., SAHOO S., PRADHAN D.K., KATIYAR R.S., *J. Appl. Phys.*, 115 (2014), 243904.

Received 2014-06-19

Accepted 2015-01-12